

# Virus removal in ceramic depth filters based on diatomaceous earth

## Supporting Information

Benjamin Michen <sup>1,2</sup>, Fabian Meder <sup>1</sup>, Annette Rust <sup>3</sup>, Johannes Fritsch <sup>4</sup>,  
Christos Aneziris <sup>2</sup> and Thomas Graule <sup>1,2</sup>

<sup>1</sup> Laboratory for High Performance Ceramics, EMPA, Swiss Federal Laboratories for Materials  
Science and Technology, Ueberlandstrasse 129, 8600 Duebendorf, Switzerland.

<sup>2</sup> Institute for Ceramics, Glass and Construction Materials, Technical University Bergakademie  
Freiberg, Agricolastrasse 17, 09596 Freiberg, Germany.

<sup>3</sup> Bachema AG, Ruetistrasse 22, 8952 Schlieren, Switzerland.

<sup>4</sup> Technology and Management Faculty, University of Applied Sciences Ravensburg–Weingarten,  
Doggenriedstrasse, 88241 Weingarten, Germany.

### **Contents**

*Characteristics of the ceramic filter candle*

*Propagation and enumeration of the bacteriophages*

*Wild type phage - the 'Siphophage'*

*Tap water details*

*Calculation of Hamaker constants*

*Colloidal characterisation of bacteriophages*

*Values for (X-)DLVO calculations*

*MS2 removal at pH 9*

*Control batch experiment*

## **Characteristics of the ceramic filter candle**

**Table S-1:** A compendium of the diatomaceous earth based filter candle characteristics. More details can be found elsewhere (Michen et al. 2011).

Table S-1. Characteristics of the ceramic filter candle	
Type	Depth filter
Major ingredient	Diatomaceous earth (DE; amorphous and crystalline silica > 80 %)
Length (mm)	119 ± 2
Inner diameter (mm)	35 ± 2
Outer diameter (mm)	50 ± 2
Filter weight (g)	89± 3
Porosity (v%) <sup>1</sup>	64 ± 6
Pore volume (ml)	86 ± 5
Mean pore diameter (µm) <sup>1</sup>	3.2 ± 0.2
Specific surface area (m <sup>2</sup> /g) <sup>2</sup>	2.1 ± 0.1
Flux at 3 bar and 25°C (m/h)	6.8 ± 1.3
Isoelectric point in 4 mM NaCl <sup>3</sup>	< 2 (if any)

<sup>1</sup> Obtained by mercury intrusion porosimetry

<sup>2</sup> according to the method of Brunauer-Emmett-Teller (BET)

<sup>3</sup> electrophoretic measurement of zeta potential as a function of pH

# 1 Propagation and enumeration of the bacteriophages

2 We chose two bacteriophages, namely *Enterobacteria* phage MS2 (MS2) and  
 3 *Enterobacteria* phage PhiX174 (Phi) that have been frequently used to  
 4 investigate virus adsorption to surfaces. Both viruses are coliphages, i.e. they  
 5 infect host bacteria of the species *Escherichia coli* (*E. coli*). However, the phages  
 6 specifically infect two different *E. coli* strains. The bacteriophages MS2 (DSM  
 7 13767) and Phi (DSM 4497) were obtained from the German Collection of  
 8 Microorganisms and Cell Cultures (DSMZ, Germany) and some of their  
 9 properties are listed in Table S-2.

**Table S-2. Properties of the bacteriophages MS2 and Phi**

	<b>MS2</b>	<b>Phi</b>
Family <sup>1</sup>	Leviviridae	Microviridae
Genus <sup>1</sup>	Levivirus	Microvirus
Species <sup>1</sup>	<i>Enterobacteria phage MS2</i>	<i>Enterobacteria phage ΦX174</i>
Nucleic acid <sup>1</sup>	ssRNA	ssDNA
Host <sup>2</sup>	<i>E. coli</i> , F-specific	<i>E.coli</i> , <i>Salmonella typhimurium</i> ;
Burst size * <sup>3</sup>	100 - 20,000	73 - 441
Morphology <sup>1</sup>	Non-enveloped; icosahedral d≈25 nm	Non-enveloped; icosahedral d≈26 nm
Molecular weight (Mega Dalton) <sup>4,5</sup>	3.6	6.2
IEP [mean ± standard deviation] <sup>6</sup>	3.5 ± 0.6	6.2 ± 1.6

10 References: <sup>1</sup> ICTVdB 2009; <sup>2</sup> Leclerc et al. 2000; <sup>3</sup> Ackermann and DuBow 1987; <sup>4</sup> Overby et al.  
 11 1966; <sup>5</sup> Sinsheimer 1959; <sup>6</sup> Michen and Graule 2010. \* Burst size: A measure of viral replication  
 12 expressed as infectious units generated per infected cell. For example, a burst size of 1,000  
 13 would indicate that 1,000 progeny viruses were generated by each initially infected cell.

14 The enumeration took place by counting plaques on lawns of bacteria in Petri  
 15 dishes. The bacteria strains used for the specific enumeration of the phages MS2  
 16 and  $\phi$  were obtained from the American Type Culture Collection (ATCC): *E. coli*  
 17 HS(pFamp)R/Famp (ATCC 700891) and *E. coli* CN-13 (ATCC 700609) for MS2  
 18 and Phi, respectively. Dilution series of the phage suspensions were performed  
 19 in 0.02 M MgCl<sub>2</sub>/0.15 M NaCl solutions in 10-fold steps. A sample volume of 4.5  
 20 ml containing phages was mixed at 25°C with 0.5 ml of phage-specific host  
 21 culture, grown at 37°C for 4 h in 30 g l<sup>-1</sup> of sterile tryptic soy broth (TSB; Oxoid,  
 22 UK), and placed into a water bath at 46°C for two to three minutes.

1 Subsequently, 5 ml of a phage-specific nutrient agar (46°C) was added into the  
2 test tube. The ingredients were mixed prior to pouring them into the Petri dish (9  
3 cm in diameter) and finally incubated at 37°C for 12 to 16 h. The concentration of  
4 agar may alter the enumeration results due to the change in viscosity (Abedon  
5 and Culler 2007). However, unequal concentrations of agar were chosen for the  
6 two phages as the plaque size of Phi and MS2 showed a great variance which  
7 made plaque counting impractical at identical agar concentrations. Reliable  
8 results were obtained for Phi with 80 g l<sup>-1</sup> tryptic soy agar (TSA) (Oxoid, UK),  
9 revealing a turbid plaque of a diameter in the range of 3 < d < 10 mm. MS2  
10 produced smaller, clear plaques between 1 < d < 5 mm at 40 g l<sup>-1</sup> TSA  
11 supplemented by 15 g l<sup>-1</sup> TSB to balance the nutrient concentration. Upper and  
12 lower limits of PFUs per plate were considered between 15 and 150 as well as  
13 between 8 and 80 for phage MS2 and Phi, respectively. The error of plating was  
14 investigated as relative error of numerous parallel samples and found to be 20%.  
15 Further platings were performed once and are reported using the established  
16 error. To assure the test's accuracy, the entire dilution series of the water sample  
17 was always plated and evaluated for conformity.

18 The propagation of bacteriophages was carried out with two different strains of *E.*  
19 *coli* obtained from the DSMZ. The two strains were DSM 5210 and DSM 13127  
20 for the replication of F-specific phage MS2 and the somatic phage Phi,  
21 respectively. All bacterial cultures produced in this work were grown for 20 h in  
22 an incubator at 37°C. From these overnight cultures, 100 µl of each was  
23 inoculated in 50 ml of TSB and incubated for 4 h at 37°C in order to obtain  
24 bacterial working cultures that emerged in an exponential growth phase. Such  
25 cultures showed typical concentrations, expressed in colony forming units (CFU),  
26 of about 10<sup>9</sup> CFU ml<sup>-1</sup>. With the goal of removing contaminating agents from the  
27 future virus stock, two principal approaches have been used with which to modify  
28 the standard propagation procedure:

- 29 • Washing: The host culture (exponential growth phase) was washed to  
30 remove low molecular agents of the complex TSB medium in which the

1 bacteria had been grown. To do this, the 4 h culture was centrifuged  
2 (3000g, 30 min) and the greenish-yellow supernatant containing the  
3 growth medium was discarded. The bacteria were re-suspended in 50 ml  
4 salt solution with 0.02 M  $\text{MgCl}_2$  and 0.15 M NaCl and placed back into the  
5 water bath at 37°C for phage inoculation.

6 • Dialysis: This step was added following the actual propagation procedure.  
7 The virus suspension was dialysed using a simple ready-to-use device  
8 equipped with a 100 kDa cellulose ester membrane (Float-A-Lyzer G2,  
9 Spectrum Laboratories Inc., USA) that also enabled the removal of  
10 dissolved salts. Therefore, 10 ml of virus suspension were subsequently  
11 dialysed twice against 1000 ml of pure water for 5 days at 4°C.

12 The host culture contained about  $10^9$  CFU  $\text{ml}^{-1}$  as no loss of bacterial vitality was  
13 observed following the washing step (data not shown). Next, the bacteriophages  
14 were added at 37°C for MS2, and at 46°C for Phi. The phage to bacterium ratio  
15 was adjusted to be close to unity and any suspension was incubated for 3-4 h.  
16 Any prepared virus stock was cleared of bacterial debris by filtration through  
17 sterile 0.45 and subsequently 0.2  $\mu\text{m}$  syringe filters. Finally, aliquots of virus  
18 suspensions were stored at 4°C.

19

## **Wild type phage - the 'Siphophage'**

While working with bacteriophage Phi, different plaque morphologies in a single Petri dish had been noticed, as shown in Figure S-1. The larger plaques appeared turbid whereas the smaller ones were clear. The white dots found inside the larger plaque were responsible for the turbid appearance and arose from phage-resistant bacteria colonies. As such colonies were found in a random fraction of plaques in a single Petri dish, this may have indicated that two different virus types were present which possessed diverse phage-host behaviour. Further, these two morphologies could be correlated with differential retention behaviour in filtration units which led to the hypothesis that two virus types were present in the stock.

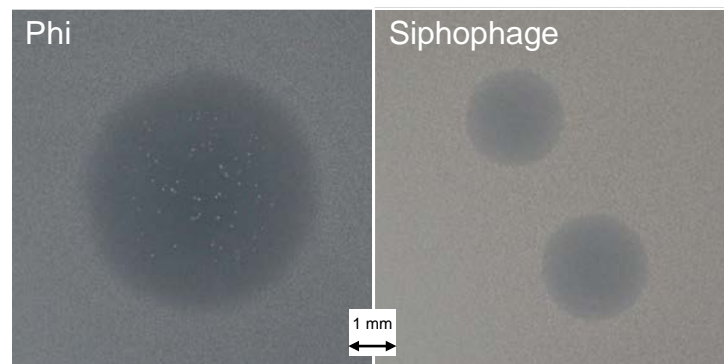
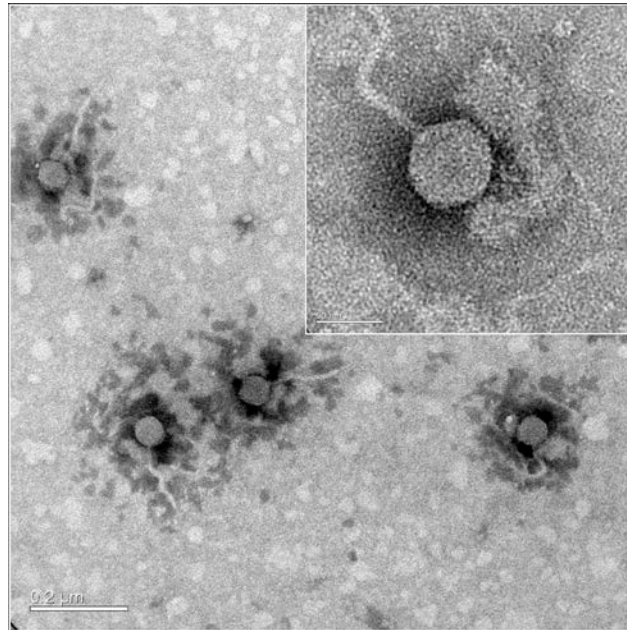


**Figure S-1.** Different plaque morphologies found in contaminated  $\phi$  virus stocks.

Plaques of both morphologies were isolated from a single Petri dish and propagated independently to obtain pure virus stocks containing either of the two virus types. When the titres of these virus stocks were determined, the two plaque morphologies could be successfully separated and hence appeared to be isolated in each virus stock. Yet, the difference in retention behaviour was observed with tests using either of the two virus stocks. This provided evidence for the assumption that the two virus types co-existed in the primary virus stock. This could be due to mutations of the phages altering their properties or another phage species which had contaminated the primary virus stock. These two phage stocks were then subjected to characterisation using transmission electron

1 microscopy (TEM) which revealed two clearly diverse bacteriophage  
2 morphologies: the expected morphology of Phi as well as an unexpected  
3 complex morphology of a tailed bacteriophage, given in Figure S-2. As the  
4 phage's morphology differed greatly from that of Phi, this could not be explained  
5 solely by mutation and thus led to the identification of a viral contaminant.



6  
7 **Figure S-2.** TEM images of the contaminant termed Siphophage.

8 This unknown contaminant showed an icosahedral head with an estimated  
9 diameter of 60 nm and a non-contractile, flexible tail with a length of about 160  
10 nm and a width of 10 nm. Due to the morphology, this phage was assigned to the  
11 T-series of bacteriophages fitting best with the dimensions of the *Enterobacteria*  
12 *phage T1* of the family Siphoviridae. This species has been known to  
13 contaminate laboratories as it remains stable there for weeks in the form of  
14 aerosols (Calendar 2006). On the other hand, this viral contaminant may have  
15 derived from a temperate phage, such as the *Enterobacteria phage λ*, which has  
16 been introduced into the genetic code of some *E.coli* strains (Calendar 2006).  
17 The prophage might have been triggered to become virulent whilst a number of  
18 propagation methods were performed and could have been established in

1 parallel to the phage Phi. Some properties of the phages that potentially could be  
2 assigned as the contaminant are listed in Table S-3. However, no other  
3 properties could be identified which allowed to us to distinguish further between  
4 the two candidates, and hence the viral contaminant is referred to as the  
5 'Siphophage' as both candidates belong to the family of Siphoviridae.

**Table S-3. Potential candidates for the viral contaminant**

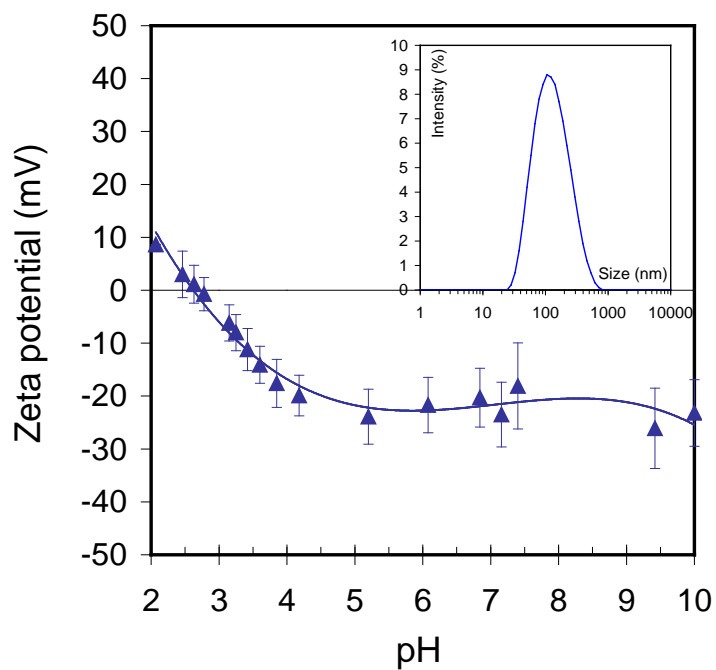
	$\lambda$	T1
Family <sup>1</sup>	Siphoviridae	Siphoviridae
Genus <sup>1</sup>	" $\lambda$ -like viruses"	"T1-like viruses"
Species <sup>1</sup>	<i>Enterobacteria phage <math>\lambda</math></i>	<i>Enterobacteria phage T1</i>
Nucleic acid <sup>1</sup>	dsDNA	dsDNA
Host <sup>2,1</sup>	<i>E.coli</i> , <i>Salmonella typhimurium</i> ; somatic	Bacteria, genus <i>Escherichia</i>
Burst size <sup>3,4</sup>	50-100	180
Morphology <sup>3</sup>	Complex; icosahedral-head with a diameter of 60 nm having a non-contractile tail with a length of 150 nm and a diameter of 10 nm.	Complex; icosahedral-head with a diameter of 60 nm having a non-contractile, flexible tail with a length of 151 nm and a diameter of 10 nm.
Molecular weight (Mega Dalton) <sup>5</sup>	60	?
IEP <sup>6</sup>	3.8 (or 2.7 in this study ?)	(2.7 in this study ?)

6 References: <sup>1</sup> ICTVdB 2009; <sup>2</sup> Leclerc et al. 2000; <sup>3</sup> Calender 2006; <sup>4</sup> Mulligan 2002; <sup>5</sup> Ackermann  
7 and DuBow 1987; <sup>6</sup> Michen and Graule 2010.

8 The Siphophage was subjected to further characterisation in terms of size and  
9 zeta potential using light scattering techniques and electrophoresis (experimental  
10 procedures are described in section S.6). The results obtained in 4 mM NaCl are  
11 shown in Figure S-3. As can be seen from the inset in the figure, the larger  
12 dimensions of the Siphophage were confirmed by size measurements of phage  
13 suspensions revealing a  $d_{\text{Hydro}}=94.4 \pm 2.6$  nm (three measurements at titres in  
14 the range from  $1.9 \cdot 10^9$  to  $7.6 \cdot 10^9$  PFU/ml). Due to the complex morphology of  
15 the phage, the determination of a hydrodynamic diameter was difficult. However,  
16 one would expect a diameter larger than the icosahedral head of the phage (60  
17 nm) and smaller than the maximum length of the phage (head and tail), which  
18 was about 210 nm long. Hence, the  $d_{\text{Hydro}}$  corresponded well with the phage size  
19 determined by TEM. The zeta potential in 4 mM NaCl as a function of pH is  
20 shown in Figure S-3. Under such conditions, the zeta potential had values of  
21 about -20 mV at neutral pH. The IEP of the Siphophage was determined to be



1 equal to pH 2.7. In the literature, only one IEP value for phage lambda at pH 3.8  
2 has been reported and none for the phage T1, making further assignment to  
3 either of the two species not feasible.



4

5 **Figure S-3.** Zeta potential as a function of pH of the Siphophage as well as the size distribution  
6 shown in the inset; all conducted in 4 mM NaCl.

7

1 **Tap water details**

2 **Table S-4:** Ion concentrations in mg/l according to a report (24.09.2007) obtained from the water  
 3 supply in Wallisellen. The table includes the conversion to ionic strength.

<b>Table S-4 Ionic conditions found in Swiss tap water near Zurich.</b>			
<b>Ion [i]</b>	<b>Cm (mg/l)</b>	<b>C (mol/l)</b>	<b><math>C_i \cdot z_i^2</math> (mol/l)</b>
Mg <sup>2+</sup>	17	0.0007	0.0028
Na <sup>+</sup>	4.5	0.0002	0.0002
Ca <sup>2+</sup>	113.8	0.0028	0.0114
Cl <sup>-</sup>	16.1	0.0005	0.0005
NO <sub>3</sub> <sup>-</sup>	23.3	0.0004	0.0004
SO <sub>4</sub> <sup>2-</sup>	26.5	0.0003	0.0011
<b>Ionic strength (I):</b>			
<b>I (M)</b>	<b>I (mM)</b>		
0.0081	<b>8.1424</b>		

4

5

## **Calculation of Hamaker constants**

**Table S-5:** The table lists some values of the Hamaker constant taken from the literature and calculated for systems which are of interest in this work. The upper part of the table lists values of like materials across air (vacuum) or water. In the lower section, Hamaker constants are given for asymmetric materials in water. According to equation S-1, the calculations were performed for two viruses, namely Tobacco mosaic virus (TMV) and MS2. The refractive index of bacteriophage MS2 has been determined by Balch et al. (2000) with  $n=1.11$  and  $\epsilon=4$  was assumed for icosahedral viruses as done by Reddy et al. (1998). For TMV, values of  $n=1.57$  and  $\epsilon=55$  were used according to Lee et al. (2008) to calculate the Hamaker constant.

Since these calculations underlie some simplifications, an average from those values available (indicated in the box in Table S-5) for viruses, or materials which are thought to have similar  $A_H$  (polystyrene, BSA; bovine serum albumin), was taken to determine a non-specific average value of  $A_H$  for viruses in air, resulting in  $A_H=11.4 \times 10^{-20}$  J. This value was transferred to an  $A_H$  which refers to the virus-water-virus system using equation S-2.

Based on this value, together with the Hamaker constant of the filter media ( $\text{SiO}_2$ ), the calculation of the asymmetric  $A_H$  between the virus and the potential adsorbent in water was performed with equation S-3. Those values that are of interest in this work are listed in Table S-5 and marked blue. Previously reported  $A_H$  values, e.g. such that have been applied to account for viral sorption processes, are given for comparison.

### **Equation S-1:**

$$A_H = \frac{3}{4} kT \left( \frac{\epsilon_{r(b)} - \epsilon_{r(m)}}{\epsilon_{r(b)} + \epsilon_{r(m)}} \right)^2 + \frac{3h\nu_e}{16\sqrt{2}} \left( \frac{(n_b^2 - n_m^2)^2}{(n_b^2 + n_m^2)^{\frac{3}{2}}} \right)$$

A widely used model capable of calculating  $A_H$  for like bodies (b) in a medium (m) according to Israelachvili (1992). Thereby, only the refractive index (n) and the relative permittivity ( $\epsilon_r$ ) of the like bodies and the media, the Plank's constant ( $h$ ) and the main electronic absorption frequency in the UV region ( $\nu_e$ ) of the media are essential to estimate the Hamaker constant. In this work, the relation always refers to the aquatic system (w), hence  $\nu_e=3 \times 10^{15}$  1/s. However, the  $A_H$  can be easily transformed with the help of equation S-2 in order to obtain the  $A_H$  of the like bodies in a vacuum (or air) (v) (Elimelech et al. 1995). This is of interest when the Hamaker constants of two different materials #1 and #2 in water are to be determined using the relation in equation S-3 (Israelachvili 1992).

#### Equation S-2:

$$A_{1w1} = \left( \sqrt{A_{1v1}} - \sqrt{A_{www}} \right)^2$$

#### Equation S-3:

$$A_{1w2} = \left( \sqrt{A_{1v1}} - \sqrt{A_{www}} \right) \cdot \left( \sqrt{A_{2v2}} - \sqrt{A_{www}} \right)$$

Table S-5. Hamaker constants ( $A_H$ )		
Material#1 across air or water	$A_H$ ( $10^{-20}$ J) air/water	Reference
Water	5.7/-	Roth and Lenhoff 1996
Polystyrene (=virus) <sup>+</sup>	6.15 to 6.6/-	Murray and Parks 1980
Polystyrene latex particles	8.4/0.9	Roth and Lenhoff 1996
BSA	9.6/1.28	Roth and Lenhoff 1996
TMV	13/1.48	this study
MS2	13.7/1.71	this study
<a href="#">Virus average value</a>	<a href="#">11.4/0.97</a>	<a href="#">this study</a>
SiO <sub>2</sub> (silica, amorphous)	6.5/0.46	Bergström 1997
SiO <sub>2</sub> (quartz, trigonal)	8.9/1.02	Bergström 1997
Material#1 – Water – Material#2	$A_H$ ( $10^{-20}$ J) system	Reference
<a href="#">Virus-water-SiO<sub>2</sub>*</a>	<a href="#">0.37</a>	<a href="#">this study</a>
Virus-water-quartz	0.33 to 0.49	Murray and Parks 1980
BSA-water-SiO <sub>2</sub> (quartz)	0.68	Roth and Lenhoff 1996

<sup>+</sup> Murray and Parks assumed that poliovirus possesses a comparable  $H_A$  to polystyrene;

\* assuming a SiO<sub>2</sub> composition of half amorphous and half trigonal;

Bovine serum albumin (BSA), Tobacco mosaic virus (TMV).

## **Colloidal characterisation of bacteriophages**

### **Experimental**

The hydrodynamic diameter ( $d_{\text{Hydro}}$ ) of the virus particles in suspension was investigated by dynamic light scattering (DLS). We used a Zetasizer Nano ZS (Malvern Instruments, UK), equipped with a laser light source (He-Ne;  $\lambda=633$  nm) to illuminate the sample suspension. Thanks to the Brownian motion of the particles, the intensity of the scattered light fluctuated with time. The DLS equipment recorded an intensity correlation curve from which the diffusion coefficient ( $D$ ) as well its distribution could be calculated. Knowing  $D$ , the  $d_{\text{Hydro}}$  could be computed with the help of the Stokes-Einstein equation (equation S-4), where  $\eta$  refers to the viscosity of the solution (water). Experiments were driven by Dispersion Technology Software (Version 5.03), which gave particle size distributions (PSD) expressed as percentage fraction of intensity as a function of particle size. Additionally, the software calculated the  $d_{\text{Hydro}}$  based on the assumption that the sample showed a monomodal distribution.

#### **Equation S-4:**

$$D = \frac{k \cdot T}{3 \cdot \pi \cdot \eta \cdot d_{\text{Hydro}}}$$

The surface charge of the phages in terms of the zeta potential ( $\zeta$ ) was determined using a microelectrophoresis system which was incorporated into the Zetasizer Nano ZS. The movement of charged particles in an alternating electrical field was determined by the frequency shift between a reference laser beam and the light which was scattered by the moving particles (Doppler Effect). Based on the frequency shift, the particle's velocity ( $v$ ) could be determined. The electrophoretic mobility ( $\mu_E$ ) of the particles could be calculated under consideration of the applied electrical field ( $E$ ), equation S-5. The  $\mu_E$  could be converted into the  $\zeta$  with the help of the equation derived by Henry (Shaw 1992) (equation S-5, term on the right hand side). This takes into account the electric

permittivity of a vacuum ( $\varepsilon_0$ ), the relative permittivity of the suspension media ( $\varepsilon_r$ ), the viscosity of the suspension ( $\eta$ ) as well as the Henry function ( $f(\kappa a)$ ), with  $a$  as the particle radius and  $\kappa$  as the Debye-Hückel parameter, given in equation S-6 (Adamczyk 2003).  $f(\kappa a)$  has a value between 1 (Hückel approximation; for  $\kappa a \ll 1$ ) and 1.5 (Smoluchowski approximation; for  $\kappa a \gg 1$ ) (Shaw 1992). The Debye-Hückel parameter takes into account the ionic strength ( $I$ ), elementary charge ( $e$ ) as well as Avogadro's number ( $N_A$ ). Further,  $\varepsilon_0$  is the electric permittivity in vacuum and  $\varepsilon_w$  is the dielectric constant of water,  $k$  refers to the Boltzmann constant and  $T$  to the absolute temperature. The inverse  $\kappa$  is also used to describe the thickness of the EDL. The software supplied by Malvern also drove the experiments performed here. Clear disposable capillary cells (DTS 1060, Malvern Instruments, UK) were used and connected with the autotitrator MPT-2 (Malvern Instruments, UK) in order to determine zeta potential ( $\zeta$ ) as a function of titrant (e.g. acid: HCl and base: NaOH to adjust pH). The measurements were done in salt solutions of NaCl with  $I = 4$  mM.

#### Equation S-5:

$$\mu_E = \frac{v}{E} = \frac{2 \cdot \varepsilon_0 \cdot \varepsilon_r \cdot \zeta \cdot f(\kappa a)}{3 \cdot \eta}$$

#### Equation S-6:

$$\kappa = \left( \frac{2 \cdot e^2 \cdot N_A \cdot I}{\varepsilon_0 \cdot \varepsilon_w \cdot k \cdot T} \right)^{\frac{1}{2}}$$

## Results

The  $d_{\text{Hydro}}$  of MS2 was determined by DLS measurements of subsequently in NaCl ( $I=4\text{mM}$ ) diluted suspensions. Three dilutions led to final titres of  $1.4 \cdot 10^{10}$ ,  $7 \cdot 10^9$  and  $3.5 \cdot 10^9$  PFU  $\text{ml}^{-1}$ . Further dilutions below  $1 \cdot 10^9$  PFU  $\text{ml}^{-1}$  gave

unreliable results accompanied by deficient measurement quality reports given by the operating software. However, measurements of these three different concentrations yielded a mean value with a standard deviation of  $d_{\text{Hydro}}(\text{MS2})=33.4 \pm 1.3$  nm. In contrast, a  $d_{\text{Hydro}}(\text{Phi})=87.9$  nm was determined for the phage Phi in a suspension with a titre of  $2.8 \times 10^9$  PFU  $\text{ml}^{-1}$ . Further dilution of the suspensions gave also unreliable results indicating that the light detector was working in the range of the detection limit (i.e. not sufficient light is scattered at suspended matter in the sample). In Figure S-4, we show the PSD of the two phages. While the scattered intensity of MS2 suspensions revealed an almost monomodal PSD, the Phi suspension showed a bimodal distribution (the relatively small peaks, in terms of intensity, at the micron scale found in both samples are neglected in this context as those are probably due to insignificant amounts of contaminants).

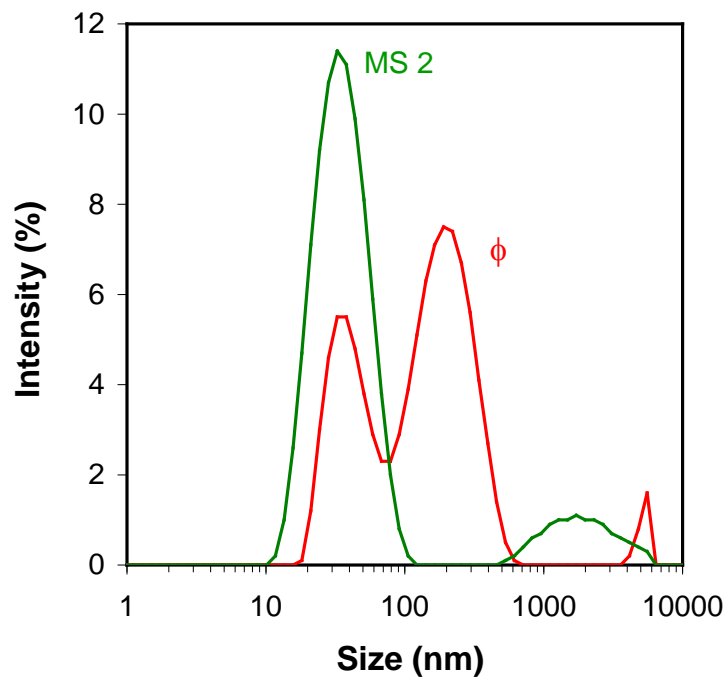
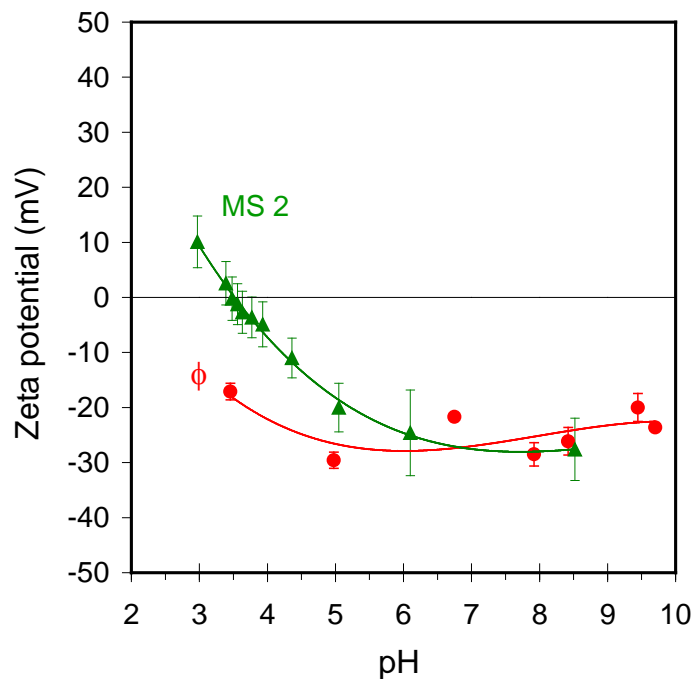


**Figure S-4.** Particle size distributions (PSD) determined by laser scattering for MS2 and Phi( $\phi$ ) in NaCl,  $I = 4$  mM at pH 7.

1 The  $\zeta$  as a function of pH were measured using MS2 and Phi samples taken from  
2 the same stock as used for the size measurements. The results are presented in  
3 Figure S-5. In the case of MS2, the surface charge in terms of the  $\zeta$  carried a net  
4 negative charge in the pH region of most naturally-occurring water sources ( $5 <$   
5  $\text{pH} < 9$ ). The IEP of bacteriophage MS2 was determined at pH 3.5. The sample  
6 containing phage Phi showed a net negative  $\zeta$  in the pH range under  
7 investigation ( $3 < \text{pH} < 10$ ) and no IEP could be detected.



8

9 **Figure S-5.** Zeta potential ( $\zeta$ ) of suspensions containing bacteriophages MS2 and  $\phi$  as a function  
10 of pH in NaCl;  $I = 4$  mM.

## 11 Discussion

12 With our measurements we could define a benchmark of  $1 \cdot 10^9$  PFU  $\text{ml}^{-1}$  as a  
13 minimum phage concentration necessary for the detection by light scattering  
14 techniques. It is suspected that this minimum titre will be needed for any virus  
15 type of similar size and molecular weight. In contrast, lower minimum  
16 concentrations would be expected for viruses with larger physical dimensions



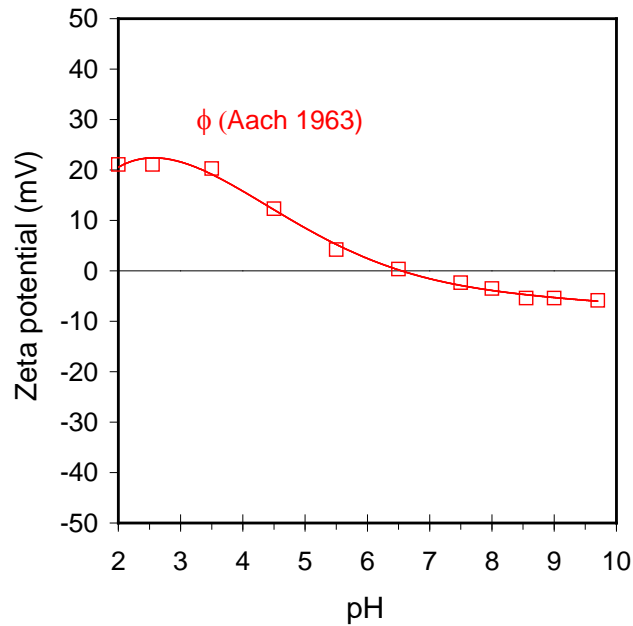
1 and mass. Measuring the hydrodynamic diameter of phage MS2 resulted in a  
 2 relatively low standard deviation that indicated high reproducibility of the  
 3 measurement. The  $d_{\text{Hydro}}(\text{MS2})$  of  $33.4 \pm 1.3$  nm was significantly larger than the  
 4 viral diameter of 25 nm as reported in Table S-2. The size of particular matter in  
 5 the aquatic environment may differ from the dry state which is often investigated  
 6 by transmission electron microscopy (TEM). This is because of the EDL at the  
 7 interface of the particle. Hence, the virus size plus the EDL thus make up the  
 8  $d_{\text{Hydro}}$ . Our results are in accordance with this formation of an EDL. Its thickness  
 9  $\kappa^{-1}$  under the experimental conditions could be calculated to be equal to 4.8 nm  
 10 (equation S-6). This resulted in a theoretical hydrodynamic diameter,  $d_{\text{Th-Hydro}}$   
 11  $d_{\text{Hydro}}(\text{MS2})$ , of 34.6 nm that was within the standard deviation of the experimental  
 12 result. In contrast, the  $d_{\text{Hydro}}$  of bacteriophage Phi measured with 87.9 nm was  
 13 out of the range of expectation as the phage's diameter of 27 nm was confirmed  
 14 by TEM investigation, see Table S-2. The DLS measurement was conducted in  
 15 the same electrolyte as the phage MS2 ( $I=4$  mM NaCl), thus a comparable  $\kappa^{-1}$   
 16 was expected. Clarification was given with the PSD of the two phages in Figure  
 17 S-4. While the scattered intensity of MS2 suspensions revealed an almost  
 18 monomodal PSD, the Phi suspension showed a bimodal distribution. The smaller  
 19 peak of the bimodal PSD could be attributed to monodisperse  $\phi$  bacteriophages,  
 20 as the peak position corresponded well with the  $d_{\text{Th-Hydro}}(\phi)=36.6$  nm based on  
 21 TEM investigation. The second, and more pronounced peak, however, may have  
 22 arisen from either contamination or viral aggregation. Suspended colloidal matter  
 23 having an IEP near the pH of the suspension media tends to form aggregates.  
 24 This has been shown for the phage MS2 which forms aggregates with sizes of a  
 25 few micrometres for  $\text{pH} \leq \text{IEP}$  (Langlet et al. 2007). Also for Phi, reversible  
 26 aggregation behaviour at close to neutral pH has been reported by Sinsheimer  
 27 (1959) which is in agreement with the reported mean IEP of 6.2 in Table S-2.  
 28 wever, Sinsheimer observed these aggregates in suspensions with high phage  
 29 concentrations ( $>9 \times 10^{13}$  PFU ml<sup>-1</sup>) only. Moreover, Sinsheimer reported  
 30 complete dispersion of virus aggregates upon dilution or increased pH. Although  
 31 the pH of the virus suspensions produced in this work was in the neutral region

1 (pH 6-7) and thus was close to the reported IEP of Phi, the titres obtained were  
2 orders of magnitude smaller than those at which aggregation had been observed  
3 in the literature. Also, it was presumed here that bacteriophage Phi might be  
4 sterically stabilised thanks to the knobs that protrude from the viral capsid  
5 (Tromans and Horne 1961). Such a steric stabilization mechanism was  
6 suggested by Penrod et al. (1996) for the phage MS2.

7 For these reasons, we suggest the presence of an organic contaminant rather  
8 than the formation of aggregates of PhiX174. Contaminants, possibly originating  
9 from bacterial debris, might have been too small to be removed in the  
10 microfiltration using 0.2  $\mu\text{m}$  syringe filters, and too large to diffuse through the  
11 dialysis membrane with a 100 kDa cut-off. It was thus suspected that the largest  
12 peak at around 200 nm of  $\phi$  in Figure S-4 could be attributed to contaminants,  
13 possibly arising from host bacteria.

14 The IEP of MS2 was determined at pH 3.5, which is equal to the average IEP  
15 value reported in the literature (Michen and Graule 2010) and confirmed the  
16 accuracy of our work. However, the sample containing phage Phi showed a net  
17 negative  $\zeta$  in the pH range under investigation ( $3 < \text{pH} < 10$ ). This was in  
18 contradiction with an expected IEP at neutral pH as has been frequently reported  
19 (Sinsheimer 1959, Aach 1963, Horká et al. 2007, Brorson et al. 2008), which  
20 would give net positive  $\zeta$  at  $\text{pH} < \text{IEP}$ . However, this confirmed the previous  
21 assumption of the presence of a contaminant which may carry a different surface  
22 charge. As the scattered intensity of Phi, recorded in the size distribution shown  
23 in Figure S-4, was largest in magnitude for the potential contaminant, this  
24 contaminant was expected to determine the signal read for the  $\zeta$  measurement  
25 as well. It is worth mentioning that, although this negative charge of phage Phi  
26 was in contradiction with the abovementioned literature, it was in agreement with  
27 other studies which determined the  $\zeta = -35$  mV at pH 6.8 (Chattopadhyay and Puls  
28 1999) and  $\zeta = -31.3$  mV at pH 7.5 (Attinti et al. 2010). However, these studies lack  
29 details on the purification of the phage suspensions prior to measurement. An

additional study, which also did not address the purification of the Phi  
 suspension, investigated the  $\zeta$  as well as the  $d_{\text{Hydro}}$  as a function of pH resulting  
 in an  $\text{IEP}(\phi) \approx 2$  and  $d_{\text{Hydro}}$  ranging from 70 to 100 nm (Aronino et al. 2009). It is  
 thus supposed that the suspension with phage Phi produced in the recent study  
 and those, which are in agreement with the results obtained in this work, suffer  
 from significant contamination. However, reliable zeta potential values of phages  
 are needed in order to quantify the electrostatic interactions in sorption processes  
 involving viruses. Due to the fact that no reliable measurements on the surface  
 charge of bacteriophage Phi could be obtained in this work, the most trustworthy  
 work of Aach was used in order to obtain  $\zeta$  values of the phage. In the work of  
 Aach, the bacteriophages were extensively purified and demonstrated an IEP at  
 pH 6.6 in 40 mM acetate buffer (Michaelis), which had been determined by the  
 electrophoretic velocity. This velocity can be converted to the  $\zeta$  using equation S-  
 5 and assuming  $f(\kappa a) = 1.4$ , as estimated graphically from the Henry equation  
 (Shaw 1992) with  $\kappa a = 17$ . The resulting  $\zeta$  as a function of pH is displayed in  
 Figure S-6.



1 **Figure S-6.** Zeta potential values calculated for bacteriophage Phi ( $\phi$ ) as a function of pH, based  
2 on experimental data by Aach 1963.

3

1 **Values for (X-)DLVO calculations**

2 **Table S-6:** All values used for the calculation of the energy-distance curves according to (X-  
3 )DLVO theory are summarised in Table S-6.

4 \* in hard water no measurements for phages could be obtained thus values at comparable pH  
5 value in soft water were used.

6

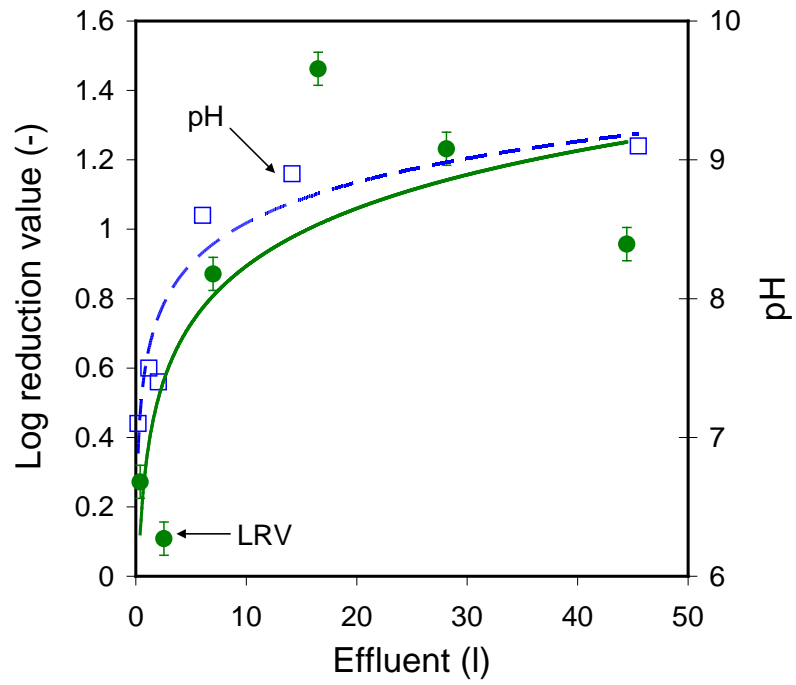
Table S-6. Values used for (X-)DLVO calculations							
	Radius		Test water conditions				
		Water-contact angle	soft water pH 5	soft water pH 6.2	soft water pH 7 (7.3)	soft water pH 9	hard water* pH 7
	r (nm)	$\theta$ (°)	$\zeta/U_{\text{Stern}}$ (mV)	$\zeta/U_{\text{Stern}}$ (mV)	$\zeta/U_{\text{Stern}}$ (mV)	$\zeta/U_{\text{Stern}}$ (mV)	$\zeta/U_{\text{Stern}}$ (mV)
<b>MS2</b>	13 <sup>1</sup>	50 <sup>2</sup>	-18/-20.1 <sup>1</sup>	-24.8/-27.8 <sup>1</sup>	-27/-30.2 <sup>1</sup>	-27/-30.2 <sup>1</sup>	-27/-30.2 <sup>1</sup>
<b>Phi</b>	14 <sup>1</sup>	42 <sup>2</sup>	9/10 <sup>1</sup>	1/1.1 <sup>1</sup>	-2/-2.2 <sup>1</sup>	-5/-5.6 <sup>1</sup>	-2/-2.2 <sup>1</sup>
<b>Siphophage</b>	42 <sup>1</sup>	96 <sup>2</sup> (82) <sup>1</sup>	-22/-24.1 <sup>1</sup>	-	-22/-24.1 <sup>1</sup>	-23/-25.2 <sup>1</sup>	-22/-24.1 <sup>1</sup>
<b>Filter</b>	-	68 <sup>3</sup>	-62/-67.4 <sup>3</sup>	-69/-75 <sup>3</sup>	-72/-78.2 <sup>3</sup>	-79/-85.8 <sup>3</sup>	-24.6/-27.7 <sup>3</sup>

7 References: <sup>1</sup> this study; <sup>2</sup> Chattopadhyay and Puls (1999); <sup>3</sup> Michen et al. 2011.

8

1 **MS2 removal at pH 9**

2 **Figure S-7:** Retention of bacteriophage MS2 in soft water at pH 9 and pH change in the effluent.



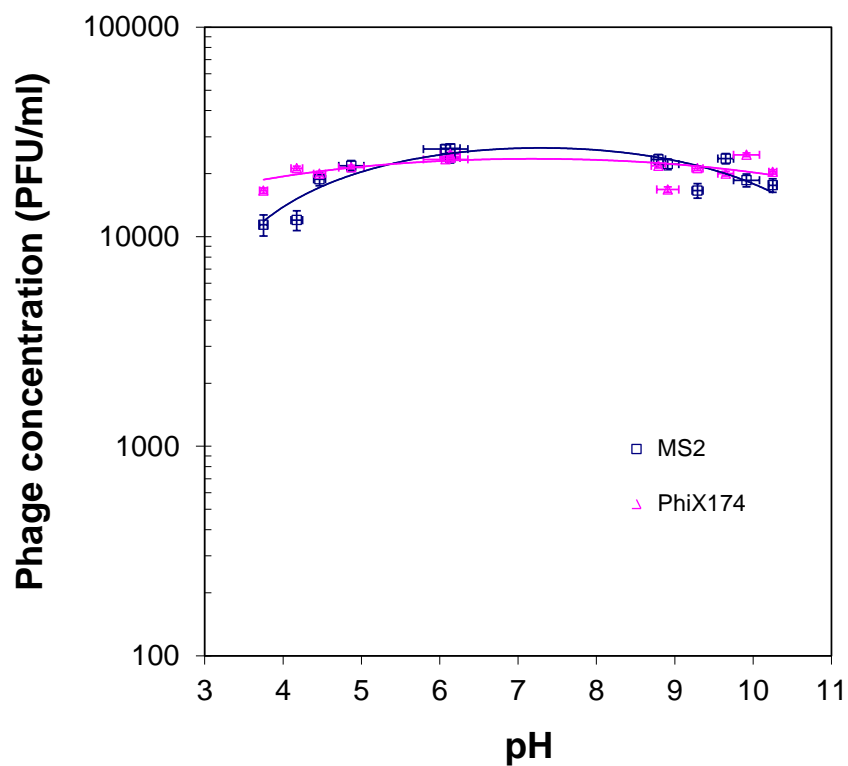
3

4

## 1 Control batch experiment

2 **Figure S-8:** The graph shows the titre of phages MS2 and PhiX174 as a function of pH in a  
3 control batch experiment. Both phages were subjected to a control experiment in which no  
4 potential adsorbent material has been added to the system. Instead the experiments were done  
5 at different pH values in order to investigate inactivation or aggregation of the phages due to pH  
6 change. The experiments were run for one hour before the sample has been filtrated and virus  
7 concentration in triplicates has been determined by enumeration.

8



9

## 1 **Reference list**

- 2 **Aach**, H.G. (1963) Elektrophoretische Untersuchungen an Mutanten des Phagen  
3 PhiX174. *Z Naturforsch B* 18, 290-293.
- 4 **Abedon**, S.T. and Culler, R.R. (2007) Bacteriophage evolution given spatial constraint. *J*  
5 *Theor Biol* 248, 111-119.
- 6 **Ackermann**, H. W. and DuBow M. S., (1987) Viruses of prokaryotes volume 2:  
7 Natural groups of bacteriophages, CRC-Press.
- 8 **Adamczyk**, Z. (2003) Particle adsorption and deposition: role of electrostatic  
9 interactions. *Adv Colloid Interfac* 100-102, 267-347.
- 10 **Aronino**, R., Dlugy, C., Arkhangelsky, E., Shandalov, S., Oron, G., Brenner, A. and  
11 Gitis, V. (2009) Removal of viruses from surface water and secondary effluents by sand  
12 filtration. *Water Res* 43, 87-96.
- 13 **Attinti**, R., Wei, J., Kniel, K., Sims, J. T. and Jin, Y. (2010) Virus' (MS2,  $\phi$ X174, and  
14 Aichi) attachment on sand measured by atomic force microscopy and their transport  
15 through sand columns. *Environ Sci Technol* 44, 2426-2432.
- 16 **Balch**, W. M., Vaughn, J., Novotny, J., Drapeau, D. T., Vaillancourt, R., Lapierre, J. and  
17 Ashe, A. (2000) Light scattering by viral suspensions. *Limnology and Oceanography*,  
18 45(2), 492-498.
- 19 **Bergström**, L. (1997) Hamaker constants of inorganic materials. *Advances in Colloid*  
20 *and Interface Science*, 70, 125-169.
- 21 **Brorson**, K., Shen, H., Lute, S., Perez, J.S. and Frey, D.D. (2008) Characterization and  
22 purification of bacteriophages using chromatofocusing. *J Chromatogr A* 1207, 110-121.
- 23 **Calender**, R. (2006) The bacteriophages; Chapter 7: Allan Campbell – General aspects  
24 of lysogeny; Chapter 8: John W. Little – Gene regulatory circuitry of phage Lambda;  
25 Chapter 17: G. J. German, R. Misra, A. M. Kropinski - The T1-like bacteriophages.  
26 Oxford University Press.
- 27 **Chattopadhyay**, S. and Puls, R.W. (1999) Adsorption of bacteriophages on clay  
28 minerals. *Environmental Science and Technology*, 33, 3609-3614.
- 29 **Elimelech**, M., Gregory, J., Jia, X. and Williams R.A. (1995) Particle deposition and  
30 aggregation: Measurement, modeling and simulation. Butterworth-Heinemann, Oxford  
31 UK.
- 32 **Horká**, M., Kubíček, O., Ruzicka, F., Holá, V., Malinovská, I. and Slais, K. (2007)  
33 Capillary isoelectric focusing of native and inactivated microorganisms. *J Chromatogr A*  
34 1155, 164-171.
- 35 **ICTvdB** – The Universal Virus Database (2009).  
36 <http://www.ncbi.nlm.nih.gov/ICTVdb/ICTVdB/index.htm>
- 37 **Israelachvili**, J.N. (1992) Intermolecular and surface forces, 2<sup>nd</sup> ed., Academic Press,  
38 London.
- 39 **Langlet**, J., Gaboriaud, F. and Gantzer, C. (2007) Effects of pH on plaque forming unit  
40 counts and aggregation of MS2 bacteriophage. *J Appl Microbiol* 103, 1632-1638.



- 1 **Leclerc**, H., Edberg, S., Pierzo, V. and Delattre, J. M. (2000) Bacteriophages as  
2 indicators of enteric viruses and public health risk in groundwaters. *Journal of Applied*  
3 *Microbiology*, 88, 5-21.
- 4 **Lee**, S. Y., Lim, J. S., Culver, J. N. and Harris, M. T. (2008) Coagulation of tobacco  
5 mosaic virus in alcohol–water–LiCl solutions. *Journal of Colloid and Interface Science*,  
6 324, 92-98.
- 7 **Michen**, B. and Graule, T. (2010) Isoelectric points of viruses. *Journal of Applied*  
8 *Microbiology*, 109(2), 388-397.
- 9 **Michen**, B., Diatta, A., Fritsch, J., Aneziris, C. and Graule, T. (2011) Removal of colloidal  
10 particles in ceramic depth filters based on diatomaceous earth. *Separation and*  
11 *Purification Technology* 81(1), 77-87.
- 12 **Mulligan**, M. E. (2002) Biochemistry. Lecture notes from  
13 <http://www.mun.ca/biochem/courses/3107/Lectures/Topics/bacteriophage.html>
- 14 **Murray**, J.P. and Parks, G.A. (1980) Poliovirus adsorption on oxide surfaces. American  
15 Chemical Society, Washington, D.C.
- 16 **Overby**, L.R., Barlow, G.H., Doi, R.H., Jacob, M. and Spiegelman, S. (1966)  
17 Comparison of two serologically distinct ribonucleic acid bacteriophages. II. Properties of  
18 the nucleic acids and coat proteins. *J Bacteriol* 92, 739-745.
- 19 **Penrod**, S. L., Olson, T.M. and Grant, S. B. (1996) Deposition kinetics of two viruses in  
20 packed beds of quartz granular media. *Langmuir* 12, 5576-5587.
- 21 **Reddy**, V. S., Giesing, H. A., Morton, R. T., Kumar, A., Post, C. B., Brooks, C. L. and  
22 Johnson, J. E. (1998) Energetics of quasiequivalence: Computational analysis of  
23 protein-protein interactions in icosahedral viruses. *Biophysical Journal*, 74, 546-558.
- 24 **Roth**, C. M. and Lenhoff, A. M. (1996) Improved parametric representation of water  
25 dielectric data for Lifshitz theory calculations. *Journal of Colloid and Interface Science*,  
26 179, 637-639.
- 27 **Shaw**, D. J. (1992) Introduction to Colloid and Surface Chemistry. Butherworth-  
28 Heinemann, Oxford, UK.
- 29 **Sinsheimer**, R.L. (1959) Purification and properties of bacteriophage PhiX174. *J Mol Bio*  
30 1, 37-42.
- 31 **Tromans**, W.J. and Horne, R.W. (1961) The structure of bacteriophage PhiX174.  
32 *Virology* 15, 1-7.
- 33  
34